



Shahid Chamran  
University of Ahvaz

# Journal of Applied and Computational Mechanics



Research Paper

## Spectral Methods Application in Problems of the Thin-walled Structures Deformation

Denys Tkachenko<sup>1</sup>, Yevgen Tsegelnyk<sup>2</sup>, Sofia Myntiuk<sup>3</sup>, Vitalii Myntiuk<sup>4</sup>

<sup>1</sup> Department of Aircraft Strength, National Aerospace University “Kharkiv Aviation Institute”, 17 Chkalova Street, Kharkiv, 61070, Ukraine, Email: d.tkachenko@khai.edu

<sup>2</sup> Department of Automation and Computer-Integrated Technologies, O. M. Beketov National University of Urban Economy in Kharkiv, 17 Marshala Bazhanova Street, Kharkiv, 61002, Ukraine, Email: y.tsegelnyk@kname.edu.ua

<sup>3</sup> Faculty of Applied Sciences, Ukrainian Catholic University, 17 Svientsitskohoho Street, Lviv, 79011, Ukraine, Email: myntiuk@ucu.edu.ua

<sup>4</sup> Department of Aircraft Strength, National Aerospace University “Kharkiv Aviation Institute”, 17 Chkalova Street, Kharkiv, 61070, Ukraine, Email: vitalii.myntiuk@khai.edu

Received August 25 2021; Revised October 25 2021; Accepted for publication December 07 2021.

Corresponding author: Y.Tsegelnyk (y.tsegelnyk@kname.edu.ua)

© 2022 Published by Shahid Chamran University of Ahvaz

**Abstract.** The spectral method ( $p$ -FEM) is used to solve the problem of a thin-walled structure deformation, such as a stiffened panel. The problem of the continuous conjugation of the membrane function from  $H^1$  and the deflection function from  $H^2$  was solved by modifying the “boundary” functions. Basis systems were constructed that satisfy not only the essential but also the natural boundary conditions, which made it possible to increase the rate of convergence of the approximate solution. The veracity of the results is confirmed by comparing the obtained spectral solution with the solution obtained by the  $h$ -FEM. It has been shown that the exponential rate of convergence characteristic of spectral methods is preserved if the Gibbs phenomenon is avoided. The constructed basis systems can be effectively used for solving various problems of mechanics.

**Keywords:** The spectral solution, Legendre polynomials, beam, plate, structure.

### 1. Introduction

Most of the practically important problems in deformable solid mechanics are reduced to boundary (initial boundary) value problems of mathematical physics. Exact integrals of these problems are extremely rare, so researchers have to resort to the construction of the approximate solutions [1–4]. Nowadays, there are a variety of methods and their modifications that give approximate solutions. The most common approach in engineering calculations is called the finite element method (FEM), or rather its  $h$ -version ( $h$ -FEM). In this version, the solution is refined by decreasing the element size. The method is widely used due to its versatility and the availability of advanced software (ANSYS, Nastran, Abacus, etc.).

Spectral methods (SM), the so-called analytical-numerical methods, have an undeniable advantage over  $h$ -FEM in the degree of accuracy approximate solutions to the exact one [5, 6]. So, if the  $h$ -FEM leads to algebraic convergence, then the analytic-numerical solution has exponential (infinite) convergence [7, 8]. The limited application of these methods is due to the increased requirements for the smoothness of the boundary, boundary conditions, coefficients of differential equations, and their right-hand sides. Fulfillment of these requirements guarantees infinite convergence of the approximate solution. Mostly, researchers use these methods to solve problems in simply connected domains and with homogeneous boundary conditions.

There are no such constraints in the  $p$ -version of the FEM ( $p$ -FEM) [9]. In this version, the accuracy of the solution is improved by increasing the degree of the approximating polynomial. In this paper, the  $p$ -FEM is considered to be SM, since in its latest implementations the distinction between these methods has nearly disappeared (see Section 2.1).

Analysis of the publications shows that the interest of researchers in SM in recent years has increased. It is not possible to make a critical review of the papers in which SM are involved in one way or another due to the large number of them. Therefore, a selection of papers was done amongst ones where the SM, as well as the  $p$ -version of the FEM and the spectral element method, were used to solve specific practical or test problems.

The spectral element method [10] was added to the list of considered methods because it differs from the above-mentioned only in the form of an approximating polynomial. In this method, it is also a polynomial but is given by the approximating Legendre–Chebyshev (Lagrange)–Lobatto polynomials. Methods that do not lead to the symmetric solution matrix (collocation method, Tau method, etc.) were not considered. Symmetry is quite a big boon to give it up.

The problems of thin-walled structures deformation consisting of beams, plates, and shells are reduced to systems of boundary value problems with differential operators of even order ( $2m$ ), arbitrary given essential and natural boundary conditions in one- and two-dimensional domains. The number of boundary conditions corresponds to the order of the differential operator. In the transition to a weak formulation, a part of the boundary conditions remains obligatory for satisfaction, namely, only the



essential ones. At the boundary where there is a joining-up of structural elements, the number required to perform the essential boundary conditions (conjugation conditions) is equal to  $m$ . It is important that these conditions are not inhomogeneous. They are arbitrarily given functions, the form of which is found out as a solution. Therefore, the references given in Tables 1–3 were grouped based on to the order of the problem differential operator, on the domain dimension in which the differential operator is given, and on the type of used basis.

The analysis of the given references shows that the most often solved SM problems are problems with a second-order differential operator in a two-dimensional domain [11, 12, 15, 16, 18–23, 25–28, 31–33, 37–39]. This group includes all papers that use the classical method of spectral element (basis functions – row 1, Table 3), and most of the papers that use the  $p$ -version of the FEM. Problems with a fourth-order differential operator are considered less often in a two-dimensional domain [45, 47, 49–54, 57–61] and, as a rule, SM is used.

Most often, researchers use basis functions representing linear combinations of Legendre and Chebyshev polynomials (row 2, Table 3). This is due to their ease of use and the remarkable properties they possess [62].

Trigonometric functions have an advantage over polynomial functions only when their use leads to the separation of variables and obtaining an analytical solution or a decrease in the dimension of the problem. Their use is limited by the presence of the specific boundary conditions. Removing these constraints by multiplying them by functions that satisfy the boundary conditions [24] (as well as another basis of this type in row 4, Table 3) leads to a rapid increase in the number of a solution matrix conditionality. In addition, the trigonometric basis has poorer approximating properties than the polynomial one (see Section 2.1).

Usage the eigenfunctions of differential operators (row 5, Table 3) leads to well-conditioned matrices (ideally, unity matrix), which is their undoubted advantage. Assuming that the system of eigenfunctions has been built, further solution of the boundary value problem can be presented in a closed-form. But the process of obtaining eigenfunctions itself can be comparable or even more computationally complex [57] than the build of a spectral solution.

Thus, as the review of papers shows, the most common basis is the polynomial one, which is explained by its good approximating properties. But the basis used in the cited papers, as a rule, satisfy only the essential boundary conditions. The construction of a basis that satisfies both the essential and the natural boundary conditions will increase the convergence and accuracy of approximate solutions.

The mechanism for conjugation structural elements into a single structure is embedded in the boundary functions – functions that have a non-zero trace at the boundary. Such functions for two-dimensional and three-dimensional domains are obtained as a result of the tensor product of one-dimensional functions [63, 64]. In the paper [36], this algorithm was extended to a three-dimensional rectangular domain, and in paper [37] to a flat triangular one. In the paper [38], the 1D vertex modes are constructed to be orthogonal to all the interior modes, which represent the eigenvalues of the second-order operator. This allowed the authors to obtain sparse mass and stiffness matrices. Another way was proposed in the paper [53], where the inhomogeneous boundary conditions are satisfied by minimizing the squared norm of the residuals. In the paper [54], the method of spectral elements is used to solve the biharmonic Dirichlet problem with homogeneous and inhomogeneous boundary conditions, with the keep  $C^1$ -continuity condition between the elemental faces. In the paper [52], the problem of free vibration of stepped thickness rectangular plates is solved by the spectral finite element method. Sufficient accuracy is achieved by dividing the plate into 4 subdomains. The authors of the paper [6] used the Lagrange-Chebyshev-Lobatto approximating polynomials with 10 collocation points and 400 subdomains to solve the problem of a chaotic nine-dimensional Lorenz system, which allowed to obtain a significant gain in accuracy compared to the Runge-Kutta method and other methods.

**Table 1.** Classification of papers according to the order of the differential operator of the considered boundary value problem.

No. in order	The order of the differential operator	References			Quantity, pcs
		1982–2000 years	2000–2010 years	2010–2021 years	
1	2	[11–26]	[27–36]	[37–44]	34
2	4	[45–49]	[50]	[51–61]	17

**Table 2.** Classification of papers according to the domain dimension.

No. in order	Domain	References			Quantity, pcs
		1982–2000 years	2000–2010 years	2010–2021 years	
1	One-dimensional	[12–14, 24, 35, 46, 48]	[29, 30, 34]	[40, 43, 44, 61]	14
2	Two-dimensional	[11, 12, 15–23, 25, 26, 45, 47, 49]	[27, 28, 31–33, 35, 50]	[37–39, 43, 51–54, 57–60]	35
3	Three-dimensional	[15]	[35, 36, 38]	[41, 43]	6

**Table 3.** Classification of papers on the basis functions type used to build solutions.

No. in order	Basis	References			Quantity, pcs
		1982–2000 years	2000–2010 years	2010–2021 years	
1	Approximating polynomial Lagrange (Chebyshev, Legendre, Lobatto)	[11, 13, 14, 17, 20, 23, 24]	[29, 33, 34]	[39, 44, 55]	13
2	Linear combinations of Legendre polynomials (integrals of Legendre polynomials)	[15, 16, 18, 19, 21, 22, 26, 47, 49]	[28, 30, 31, 36, 50]	[40, 41, 43, 54, 59–61]	21
3	Trigonometric	[12, 48]	[32]	[51, 52, 56]	6
4	Arbitrary functions, multiplication by shape functions	[25]	[31]	[37]	3
5	Eigenfunctions of differential operators		[35]	[38, 57, 58]	4



In all the above papers, a plane or one-dimensional domain is divided into subdomains in which the same differential operator is considered. FEM solves problems in branched domains, but the differential operators in these domains also have the same order. For this, in the case of solving the problem of beams, plates, and shells structures deformation instead of classical theories, the Timoshenko type theories [65] are used, which makes it possible to reduce the order of the differential operator from four to two. In this paper, the SM is applied to solve the problem of the branched thin-walled structures deformation. The problem that is solved here is related to the differential operators of boundary value problems in neighboring domains, which are occupied by the joined elements. If they have a different order, then the number of the essential boundary conditions will be different. This difference does not lead to problems when conjugating one-dimensional elements, since the boundaries are points. Problems arise with elements on the boundary, which is the closed interval: between the faces of the elements, it is necessary to ensure the continuity condition, on the one hand, only  $C^0$ , and on the other hand, both  $C^0$  and  $C^1$ . The solution is demonstrated in the test case of a stiffened panel bending.

The difficulty of building functions with which the conjugation of structural elements is performed is one of the obstacles to the propagation of SM in the calculations of complex structures. Removing this obstacle is the main goal of this investigation. To achieve it, the tasks of building an analytical basis, building approximate solutions, verifying the obtained results by comparing with the other methods results and investigating the convergence of an approximate solution it are posed.

## 2. Problem Solution Strategy

### 2.1 To the Problem of the Choice of a Basis

If the system of functions is linearly independent, complete, and satisfies the essential boundary conditions, then it can be used as the basis. The choice of one or another basis is determined by the computational aspects. This is, first of all, the number of conditioning of the resolving matrices to which the basis leads. The larger the condition number of the matrix, the greater the rounding error. Orthonormal systems are ideal in this regard, they lead to matrices with an invariable condition number equal to 1. In addition, basis systems should have better-approximating properties, which allows less computing resources to achieve more accurate results. Let's demonstrate this with a simple example of bending simply supported plate under uniformly distributed load  $q$ . As is known [65], this problem has an exact solution:

$$w_a = \frac{16q}{\pi^6 D} \sum_{i=1,3,\dots} \sum_{j=1,3,\dots} i^{-1} j^{-1} \sin \frac{i\pi x}{a} \sin \frac{j\pi y}{b} \left( \frac{i^2}{a^2} + \frac{j^2}{b^2} \right)^{-2} \quad (1)$$

The dimensionless values of the maximum deflection, bending moment and shear force for a square plate ( $b = a$ ), respectively, are

$$w_a^{\max} = \bar{w}_a^{\max} \frac{D}{qa^4} = \frac{16}{\pi^6} \sum_{i=1,3,\dots} \sum_{j=1,3,\dots} \frac{(-1)^{\frac{i+j-1}{2}}}{ij(i^2 + j^2)^2}; M_a^{\max} = \bar{M}_a^{\max} \frac{1}{qa^2} = \frac{16}{\pi^4} \sum_{i=1,3,\dots} \sum_{j=1,3,\dots} (-1)^{\frac{i+j-1}{2}} \frac{i^2 + \nu j^2}{ij(i^2 + j^2)^2}; \quad (2)$$

$$Q_a^{\max} = \bar{Q}_a^{\max} \frac{1}{qa} = \frac{16}{\pi^3} \sum_{i=1,3,\dots} \sum_{j=1,3,\dots} \frac{(-1)^{\frac{i-1}{2}}}{j(i^2 + j^2)},$$

where  $D = Eh^3 / (12(1 - \nu^2))$  is the cylindrical stiffness;  $h$  is the plate thickness;  $E$  is the modulus of elasticity;  $\nu$  is the Poisson's ratio. In this example  $\nu = 0.3$  is taken.

In the calculation of the values (2), the upper limit of the sums ( $N$ ) is taken to be finite. With its increase, the values of  $w_N^{\max}$ ,  $M_N^{\max}$  and  $Q_N^{\max}$  will approach the exact ones. To estimate the relative error of their calculation, the following values  $w_{10}^{\max} = 0.00406235$ ,  $M_{71}^{\max} = 0.0478864$  and  $Q_{275000}^{\max} = 0.337657$  were taken as reference values. All significant digits are correct in these values, except for the last one.

For comparison, consider the approximation of the deflection by polynomial functions

$$w_p = \sum \sum W_{ij} \eta_i(x) \eta_j(y), \quad (3)$$

where

$$\eta_n = P_{n+4} - \frac{2(2n+5)((n+1)^2 + 3n+8)}{(n+1)(n+2)(2n+3)} P_{n+2} + \frac{(2n+7)(n+4)(n+3)}{(n+1)(n+2)(2n+3)} P_n. \quad (4)$$

In Eq. (3) and below, unless otherwise stated, the summation indices run from the values 0, 1, ... It should be noted that functions (4) satisfy both the essential and the natural boundary conditions of a simply supported plate and have orthogonal second derivatives in  $L_2$  [66]. Here and below, the maximum values of the displacements and stresses or their equivalents most requested from the engineering point of view are compared. The graphs of the calculation errors ( $\varepsilon$ ) dependence on the values of the maximum deflection, bending moment, and shear force on the upper limit of summation in (1) and (3) are shown in Fig. 1. As it can be seen, the convergence of polynomial solutions (3) is significantly higher than the convergence trigonometric one (1). The error in determining values of the displacements, moments, and forces by solution (3) is less than one percent is achieved at  $N = 2$  (the order of the solution matrix is four). To obtain the same accuracy using solution (1), it is necessary to keep  $N = 2$  for the deflection determination,  $N = 4$  for the moment calculation, and  $N = 16$  for the force calculation.

This illustrative example shows better approximation properties of the polynomials compared to the trigonometric functions. It makes no sense to compare the sums (1) and (3), since series (1) is a ready-made solution, while in (3) it is necessary to first determine the coefficients  $W_{mn}$ , for which it is necessary to compose and solve a system of linear algebraic equations.

Note that many numerical methods, as a result of their development, are transformed to such an extent that, in essence, they turn into other methods. Let show this by the example of  $p$ -FEM and SM. In the  $p$ -FEM, for a one-dimensional finite element from  $H^1$  (here we mean the Sobolev function space), the form functions are given in the form [63]

$$u(x) = \bar{u}_1 N_1(x) + \bar{u}_2 N_2(x) + \sum_i \bar{U}_i \varphi_i^{FEM}(x), \quad (5)$$



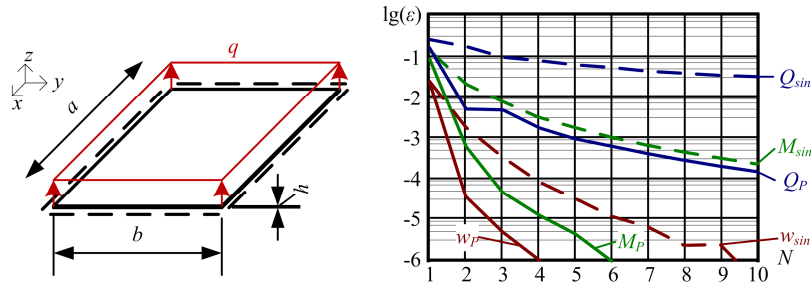


Fig. 1. Graphs of the error dependence in calculating the maximum deflection, bending moment, and shear force of a simply supported plate on the upper summation subscript N: subscript “P” is the solution approximation by polynomials (3); subscript “sin” is the solution approximation by trigonometric functions (1).

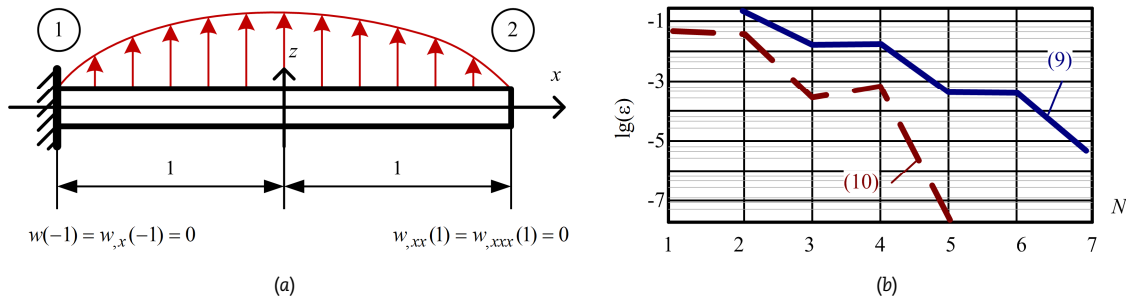


Fig. 2. Beam bending and the convergence of the maximum bending moment: (a) are the dimensions of the beam, fixing and loading scheme; (b) is the convergence of the maximum bending moment calculated from the deflections (9) and (10).

where  $\bar{u}_1, \bar{u}_2$  are the nodal displacements;  $\bar{U}_i$  are the “internal” unknown variables;  $N_1(x), N_2(x)$  are the simplex element shape functions;  $\varphi_i^{FEM}(x)$  are the functions with zero values in the nodes.

In the case of the SM application for problems with inhomogeneous boundary conditions, the function is represented in the form

$$u(x) = u_0(x) + \sum_i U_i \varphi_i(x), \tag{6}$$

where  $u_0(x)$  is the function that satisfies inhomogeneous boundary conditions. It can be expressed in the form  $u_0(x) = \bar{u}_1 N_1(x) + \bar{u}_2 N_2(x)$ , where  $\varphi_i(x)$  are called basis (coordinate) functions. They must satisfy homogeneous essential boundary conditions. As can be seen, the structures of functions (5) and (6) are identical.

In addition, in  $p$ -FEM, “internal” functions  $\varphi_i^{FEM}(x)$  (see, for example, [63, 67]) that are chosen as the Legendre polynomials integrals  $\varphi_i^{FEM}(x) = \int_{-1}^x P_{i+1}(t) dt$  ( $\psi_i^{FEM}(x) = \int_{-1}^x \int_{-1}^t P_{i+2}(s) ds dt$  are similar functions from  $H^2$ ). In the SM, basis functions from  $H^1$  and  $H^2$  are selected as linear combinations of Legendre polynomials [64, 66]

$$\varphi_i(x) = P_{i+2}(x) - P_i(x), \tag{7}$$

$$\psi_i(x) = P_{i+4}(x) - \frac{2(2i+5)}{2i+3} P_{i+2}(x) + \frac{2i+7}{2i+3} P_i(x). \tag{8}$$

Functions (7) are equal to zero at the points  $x = \pm 1$  and have orthogonal derivatives in  $L_2$ . Functions (8), in addition, have zero first derivatives at the points.

Functions (7) and (8) coincide with the  $p$ -FEM functions up to a constant:  $\varphi_i^{FEM}(x) \equiv (2i+3)\varphi_i(x)$ ,  $\psi_i^{FEM}(x) \equiv (2i+5)(2i+7)\psi_i(x)$ , i.e., with this choice of approximating functions, the difference between these two methods disappears completely.

Note that the approximating properties of a basis are improved if it satisfies not only the essential but also the natural boundary conditions. Let demonstrate this for the bending problem of a cantilever beam shown in Fig. 2,a. At the point  $x = 1$ , we have two natural conditions.

The deflection function can be represented in the classical way ( $p$ -FEM (5) or SM (6)), leaving the natural boundary conditions without satisfaction

$$w(x) = \bar{w}_2 \frac{(2-x)(1+x)^2}{4} + \bar{\theta}_2 \frac{(x-1)(1+x)^2}{4} + \sum_{n=0}^N W_n \psi_n(x), \tag{9}$$

where  $\bar{w}_2, \bar{\theta}_2$  are the unknown displacements of the right edge of the beam;  $\psi_n(x)$  is a basis that only satisfies the essential homogeneous boundary conditions (8). Or

$$w(x) = \sum_{n=0}^N W_n \vartheta_n(x), \tag{10}$$



where the basis functions [66]

$$\vartheta_n(x) = P_{n+4}(x) - \frac{4(2n+7)}{(n+2)^2} P_{n+3}(x) - \frac{2(n-1)(2n+5)(n+6)(n+4)}{(2n+3)(n+2)^2(n+1)} P_{n+2}(x) + \frac{4(n+4)^2(2n+7)}{(n+2)^2(n+1)^2} P_{n+1}(x) + \frac{(n+4)^2(2n+7)(n+3)^2}{(2n+3)(n+2)^2(n+1)^2} P_n(x),$$

satisfy all four boundary conditions and have orthogonal second derivatives in  $L_2$ .

The degree of the approximating polynomial in (10) for the same number of unknowns is two units higher than in (9), hence the better convergence of solution (10). Fig. 2,b shows the convergence of the maximum bending moment under the action of a distributed load in the form  $q(x) = \cos(\pi x/2)$ .

## 2.2 Weak Formulation of Boundary Value Problems

Below consider boundary value problems describing the deformations of thin-walled structural elements: classical beams and plates. All two-dimensional rectangular domains  $\Omega = \{(\tilde{x}, \tilde{y}) : |\tilde{x}| < a, |\tilde{y}| < b\}$  are reduced to the dimensionless domain  $\Omega = \{(x, y) : |x| < 1, |y| < 1\}$  by replacing dimensional coordinates with dimensionless ones  $x_i = \tilde{x}_i/a$  and  $y_i = \tilde{y}_i/b_i$ .

A spectral solution is built using the variational principle of the minimum of the total potential energy  $\delta\Pi = 0$ . The total potential energy  $\Pi$  consists of the deformation energy  $\Pi_\varepsilon$  and the potential of external forces. The variation of the potential energy of deformation is the sum of the element's energies variations added to the structure. In the tasks considered below, it can be:

a) variation of the energy of the plane stress in thin flat plates

$$\delta\Pi_\varepsilon^p(u, v) = b \int_{-1}^1 \int_{-1}^1 [N_x \delta u_{,x} + N_{xy} (\lambda \delta u_{,y} + \delta v_{,x}) + N_y \lambda \delta v_{,y}] dx dy, \quad (11)$$

where  $N_x = A(u_{,x} + \nu \lambda v_{,y})/a$ ,  $N_y = A(\nu u_{,x} + \lambda v_{,y})/a$ ,  $N_{xy} = A(1 - \nu)(\lambda u_{,y} + v_{,x})/(2a)$  are the forces per unit length;  $A = Eh/(1 - \nu^2)$  is the membrane stiffness;  $u, \nu$  are functions of displacements along the  $x$  and  $y$  axes, respectively;  $\lambda = a/b$  is the plate size ratio; subscripts  $x$  and  $y$  after the decimal point denote partial derivatives;

b) variation of the bending energy of a classical plate model

$$\delta\Pi_\varepsilon^b(w) = \lambda^{-1} \int_{-1}^1 \int_{-1}^1 [M_x \delta w_{,xx} - 2\lambda M_{xy} \delta w_{,xy} + M_y \lambda^2 \delta w_{,yy}] dx dy, \quad (12)$$

where  $M_x = -Da^{-2}(w_{,xx} + \nu \lambda^2 w_{,yy})$ ,  $M_y = -Da^{-2}(\lambda^2 w_{,yy} + \nu w_{,xx})$ ,  $M_{xy} = -M_{yx} = Da^{-1}(1 - \nu)\lambda w_{,xy}$  are the bending and twisting moments per unit length;  $w$  is the deflection function.

In the classical theory of plates only static values of shear forces can be determined  $Q_x = (\lambda M_{yx} + M_{x,x})/a$ ,  $Q_y = (\lambda M_{y,y} - M_{xy,x})/a$ ;

c) variation of the energy of tension-compression and bending of a classical beam

$$\delta\bar{\Pi}_\varepsilon^b(u, w) = \int_{-1}^1 [N \delta u_{,x} + M a^{-1} \delta w_{,xx}] dx, \quad (13)$$

where  $N = Ea^{-2}(Fau_{,x} - Sw_{,xx})$ ,  $M = Ea^{-2}(Iw_{,xx} - Sau_{,x})$  are the normal force and bending moment;  $F = hb$  is the beam cross-section area;  $S = Fe$ ,  $I = bh^3/12 + e^2F$  are the static and axial moments of inertia of the beam cross-section relative to the axis displaced by a distance of  $e$ .

## 2.3 Building a Basis for the Displacement Functions of Structural Elements

A function from  $H^1$  that takes nonzero values at the boundaries of the closed interval  $(-1, 1)$  can be represented in the system of basis functions

$$\zeta = \text{Span}(N_1(x), N_2(x), \varphi_n, n = 0, 1, \dots), \quad (14)$$

where  $N_1(x) = (P_0(x) - P_1(x))/2 = (1 - x)/2$ ,  $N_2(x) = (P_0(x) + P_1(x))/2 = (1 + x)/2$  are the functions of a one-dimensional simplex element shape;  $\varphi_n(x)$  is according to (7).

A function from  $H^1$  in a square region  $(-1, 1)^2$  can be expressed through the system of the basis functions obtained as a tensor product (14):

$$f(x, y) = \bar{f}_2 N_1(x) N_1(y) + \bar{f}_3 N_2(x) N_1(y) + \bar{f}_1 N_1(x) N_2(y) + \bar{f}_4 N_2(x) N_2(y) + \sum [\bar{F}_n^1 N_1(x) + \bar{F}_n^2 N_2(x)] \varphi_n(y) + \sum [\bar{F}_n^3 N_1(y) + \bar{F}_n^4 N_2(y)] \varphi_n(x) + \sum \sum F_{ij} \varphi_i(x) \varphi_j(y), \quad (15)$$

where  $\bar{f}_i$ ,  $i = \overline{1, 4}$  are the function values at the corner points  $f(\pm 1, \pm 1)$ ;  $\bar{F}_n^i$ ,  $i = \overline{1, 4}$  are the coefficients that determine the function on the edges  $f(x, \pm 1)$ ,  $f(\pm 1, y)$ ;  $F_{ij}$  are the coefficients that determine the function in the domain.

A similar representation of a function from  $H^2$  in a two-dimensional domain can be done in the system of basis functions

$$\rho(x, y) = \xi(x) \otimes \xi(y), \quad (16)$$

where

$$\xi(x) = \text{Span}(M_1(x), M_2(x), K_1(x), K_2(x), \psi_n(x), n = 0, 1, \dots); M_1(x) = (P_0(x) - P_1(x))/2 - (P_1(x) - P_3(x))/10 = (2 + x)(1 - x)^2/4,$$

$$M_2(x) = (P_0(x) + P_1(x))/2 + (P_1(x) - P_3(x))/10 = (2 - x)(1 + x)^2/4, K_1(x) = (P_0(x) - P_2(x))/6 - (P_1(x) - P_3(x))/10 = (1 + x)(1 - x)^2/4,$$

$$K_2(x) = -(P_0(x) - P_2(x))/6 - (P_1(x) - P_3(x))/10 = (x - 1)(1 + x)^2/4$$

are the Hermite cubic interpolation functions;  $\psi_n(x)$  is according to (8);  $\otimes$  is a symbol of tensor product.



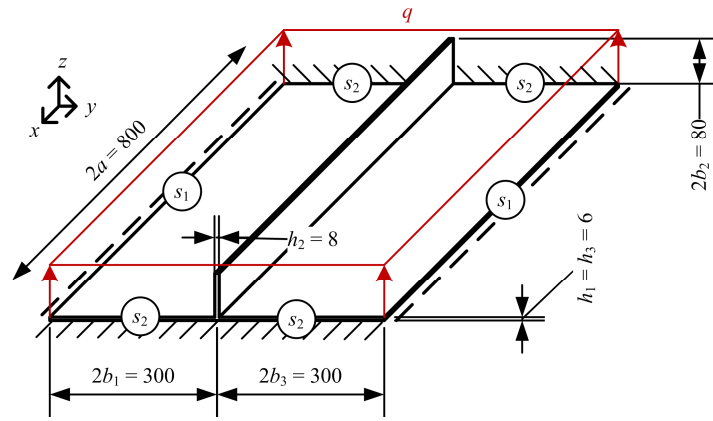


Fig. 3. Stiffened panel loaded with a uniform pressure.

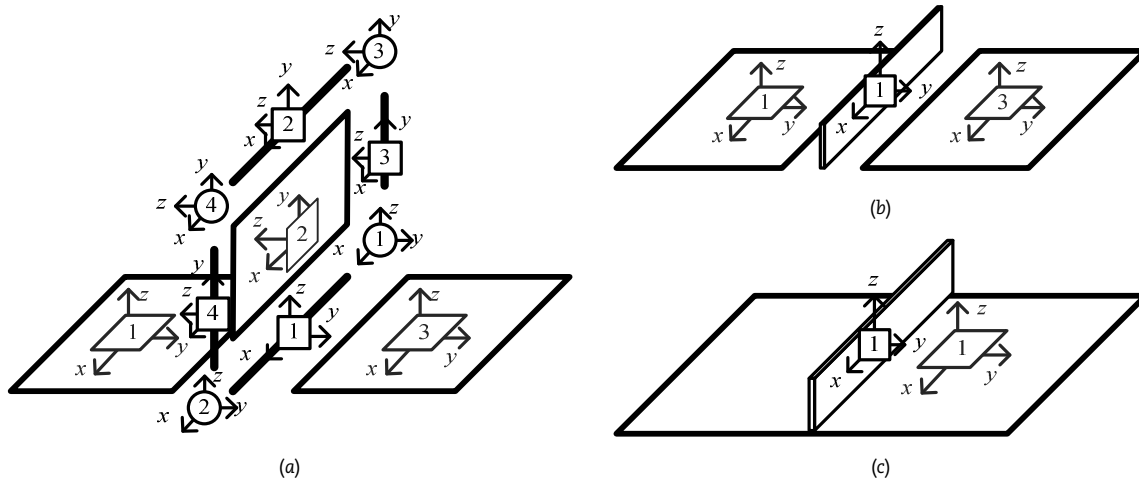


Fig. 4. Three models of stiffened panels: (a) are the three plates; (b) are the two plates and a beam; (c) is the one plate and beam.

2.4 Conjugate of Structural Elements

Conjugation of structural elements will be performed using the example of the construction of a stiffened panel (such panels are widely used in aircraft construction and are usually manufactured by machining [68–70]) shown in Fig. 3. Similar structures were considered, for example, in [71, 72]. In these papers, analytical solutions were obtained, but only bending was considered, displacements in the plane of the plate were not considered.

The simplicity of the chosen structure (in fact, only one joint is modeled) is explained by the desire to more clearly show the way of coordinating the functions of displacements on the conjugation line. The further build-up of a structure of this type by adding new elements does not present any difficulties. The displacement functions in the resulting joints are coordinated in the following way.

Dimensions in Fig. 3 are indicated in millimeters, the value of uniform pressure  $q = 0.05$  MPa, the modulus of material elasticity  $E = 72000$  MPa, Poisson's ratio  $\nu = 0.3$ . On the edges  $s_1$  simply supported are given ( $w = 0$  and  $M_y = 0$ ). On the edges  $s_2$  the clamped are given ( $w = 0$  and  $w_x = 0$ ). No conditions along the edges  $s_1$  and  $s_2$  are imposed on the displacement functions  $u$  and  $v$ . The functions  $u$ ,  $v$ , and  $w$  are built in such a way that the symmetry of the problem is considered. The panel is represented by three types of design schemes: three plates (Fig. 4,a); two plates and a beam (Fig. 4,b); one plate and a beam (Fig. 4,c).

In general, the plates have all three displacements. The deflection function for plate 1 (Fig. 4,a) is expressed through the system of functions (16)

$$w_1 = \sum \bar{W}_i^1 \psi_{2i}(x) M_2(y) + \sum \bar{\Theta}_i^3 \psi_{2i}(x) K_1(y) + \sum \sum W_{ij}^1 \psi_{2i}(x) \psi_j(y). \tag{17}$$

Here  $\bar{\Theta}_n^3$  are constants that determine the angles of the edge  $y = -1$  rotation. This function can be improved according to the remark made in subsection 2.1. On the edge  $y = -1$ , it is possible to satisfy all boundary conditions  $w_1(x, -1) = 0$  and  $M_y(x, -1) = 0$ . To do this, it is necessary to replace the function  $M_2(y)$  with  $M'_2(y) = (1 + x)(11 - 2x - x^2)/16$  and use the following instead of the basis  $\psi_i(y)$  [66]:

$$\psi_n^{sc}(y) = P_{n+4}(y) + \frac{2n+7}{(n+2)^2} (P_{n+3}(y) - P_{n+1}(y)) - \frac{(2n+5)(2(n+1)^2 + 6n+13)}{(2n+3)(n+2)^2} P_{n+2}(y) + \frac{(2n+7)(n+3)^2}{(2n+3)(n+2)^2} P_n(y). \tag{18}$$

The zero, first and second basis functions (18), their first and second derivatives are shown in Fig. 5.



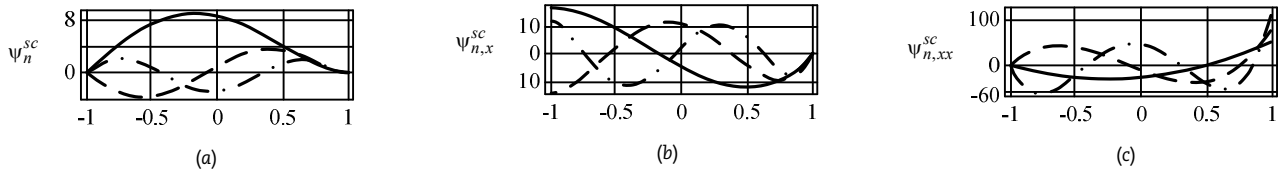


Fig. 5. The first three basis functions  $\psi_n^{sc}(y)$  and their derivatives: (a) are the functions themselves; (b) is the first derivative; (c) is the second derivative.

Thus, the resulting basis system will satisfy all the boundary conditions, including the natural ones. Finally

$$w_1 = \sum \bar{W}_n^1 \psi_{2n}(x) M_2'(y) + \sum \sum W_{ij}^1 \psi_{2i}(x) \psi_j^{sc}(y). \quad (19)$$

No essential boundary conditions are imposed on the  $u_1$  and  $v_1$  displacement functions, except for the conjugation conditions at  $y = 1$ . The  $u_1$  function is skew-symmetric with respect to the  $y$ -axis, belongs to  $H^1$ , is determined by (15)

$$u_1 = (\bar{u}_3 N_1(y) + \bar{u}_1 N_2(y))(N_1(x) - N_2(x)) + \sum \bar{U}_i^1 (N_1(x) - N_2(x)) \varphi_i(y) + \sum \bar{U}_i^3 \varphi_{2i}(x) N_1(y) + \sum \bar{U}_i^1 \varphi_{2i}(x) N_2(y) + \sum \sum U_{ij}^1 \varphi_{2i}(x) \varphi_j(y), \quad (20)$$

or easier, if basis  $\varphi_n^{f0}(y) = P_{n+1}(y) - P_n(y)$  is defined, which takes zero value at the edge  $y = 1$ ,

$$u_1 = \sum \bar{U}_{1n} P_{2n+1}(x) N_2(y) + \sum \sum W_{ij}^1 P_{2i+1}(x) \varphi_j^{f0}(y). \quad (21)$$

Unlike function  $u_1$ , function  $v_1$  is symmetric about the  $y$ -axis and takes zero value at edge  $y = 1$ , so its form is simplified:

$$v_1 = \sum \sum W_{ij}^1 P_{2i}(x) \varphi_j^{of}(y). \quad (22)$$

The displacement functions for plate 3 are built in a similar way:

$$w_3 = \sum \bar{W}_n^1 \psi_{2n}(x) M_1'(y) + \sum \sum W_{ij}^3 \psi_{2i}(x) \psi_j^{cs}(y); \quad (23)$$

$$u_3 = \sum \bar{U}_{1n} P_{2n+1}(x) N_1(y) + \sum \sum W_{ij}^3 P_{2i+1}(x) \varphi_j^{f0}(y); \quad (24)$$

$$v_3 = \sum \sum W_{ij}^1 P_{2i}(x) \varphi_j^{of}(y). \quad (25)$$

Here

$$M_1'(y) = (1-x)(11-2x-x^2)/16; \quad \varphi_n^{f0}(y) = P_{n+1}(y) + P_n(y);$$

$$\psi_n^{cs}(y) = P_{n+4}(y) - \frac{2n+7}{(n+2)^2} (P_{n+3}(y) - P_{n+1}(y)) - \frac{(2n+5)(2n+1)^2 + 6n+13}{(2n+3)(n+2)^2} P_{n+2}(y) + \frac{(2n+7)(n+3)^2}{(2n+3)(n+2)^2} P_n(y).$$

Due to the symmetry, the deflection of the second plate (Fig. 4,a) is equal to zero  $w_2 = 0$ .

Function  $u_2$  from  $H^1$  satisfies the essential boundary conditions only on edge  $y = -1$

$$u_2(x, y) = \sum \bar{U}_{1n} P_{2n+1}(x) N_1(y) + \sum \sum U_{ij}^2 P_{2i+1}(x) \varphi_j(y). \quad (26)$$

The displacement function  $v_2$  is given by the classical  $p$ -FEM method. It should be searched for in the form (15), but with such a function definition it is impossible to satisfy the conjugation conditions on the edge  $y = -1$ . The value of the function at this edge according to Eq. (15) is  $v_2(x, -1) = \sum_{n=0,1,\dots}^{N+1} \bar{V}_n^2 \varphi_{2n}(x)$ , and the corresponding displacement of axis 1 (deflection of the first plate at  $y = 1$  and the third at  $y = -1$ ) is the  $w_1(x, 1) = w_3(x, -1) = \sum_{n=0,1,\dots}^N \bar{W}_n^1 \psi_{2n}(x)$ , i.e. here it is not possible to perform conjugation by simply equating the coefficients, as it was for plates 1 and 3.

There are several ways out of this. You can still search for a solution in the form (15)

$$v_2(x, y) = \bar{v}_3 N_1(x) N_2(y) + \bar{v}_4 N_2(x) N_2(y) + \sum \sum F_{ij} \varphi_{2i}(x) \varphi_j(y) + \sum [\bar{V}_n^4 N_1(x) + \bar{V}_n^3 N_2(x)] \varphi_n(y) + \sum [\bar{V}_n^1 N_1(y) + \bar{V}_n^2 N_2(y)] \varphi_{2n}(x), \quad (27)$$

and the coefficients  $\bar{V}_n^1$  can be expressed in terms of  $\bar{W}_n^1$

$$\bar{V}_n^1 = \begin{cases} -\bar{W}_n^1 (4n+7)/(4n+3) & 2n \leq 1; \\ \bar{W}_{n-1}^1 - \bar{W}_n^1 (4n+7)/(4n+3) & 1 < 2n \leq 2N; \\ \bar{W}_{n-1}^1 & N < n \leq N+1. \end{cases}$$



The second option is to represent function  $v_2$  in the basis system (16)

$$v_2(x, y) = [\bar{v}_3 M_1(x) + \bar{v}_4 M_2(x) + \bar{\theta}_{23} K_1(x) + \bar{\theta}_{24} K_2(x)] M_2(y) + [\bar{\theta}_{y2} M_1(x) + \bar{\theta}_{y1} M_2(x)] K_1(y) + [\bar{\theta}_{y3} M_1(x) + \bar{\theta}_{y4} M_2(x)] K_2(y) + [\bar{m}_2 K_1(x) + \bar{m}_1 K_2(x)] K_1(y) + [\bar{m}_3 K_1(x) + \bar{m}_4 K_2(x)] K_2(y) + \sum [\bar{W}_n^1 M_1(y) + \bar{V}_n^2 M_2(y) + \bar{\Theta}_n^1 K_1(y) + \bar{\Theta}_n^2 K_2(y)] \psi_{2n}(x) + \sum \sum [\bar{V}_n^4 M_1(x) + \bar{V}_n^3 M_2(x) + \bar{\Theta}_n^4 K_1(x) + \bar{\Theta}_n^3 K_2(x)] \psi_n(y) + \sum \sum V_{ij}^2 \psi_{2i}(x) \psi_j(x), \tag{28}$$

where  $\bar{v}_3, \bar{v}_4, \bar{\theta}_{23}, \bar{\theta}_{24}, \bar{\theta}_{yi}, \bar{m}_i$  are the values of the function and its derivatives  $v_{,x}(\pm 1, \pm 1), v_{,y}(\pm 1, \pm 1), v_{,xy}(\pm 1, \pm 1)$  at the corner points;  $\bar{V}_n^1, \bar{\Theta}_n^1$  are the coefficients that determine the function  $v(x, \pm 1), v(\pm 1, y)$  and its derivatives on the edges  $v_{,x}(\pm 1, y), v_{,y}(x, \pm 1)$ ;  $V_{ij}$  are the coefficients that determine the function in the domain;  $\bar{W}_n^1$  are the conjugation coefficients. All other coefficients are considered free.

Thus, in both cases, the conjugation is performed by jointly using the coefficients  $\bar{U}_n^1$  and  $\bar{W}_n^1$  in functions (19), (21)–(26), and (27) or (28). The conditions for conjugation of the built functions

$$u_1(x, 1) = u_3(x, -1) = u_2(x, -1), \quad w_1(x, 1) = w_3(x, -1) = v_2(x, -1),$$

while keeping the corresponding number of terms in the sums are satisfied exactly.

In the case of using Model 2 (Fig. 4,b) for plates 1 and 3, the displacement functions are taken in the form (19), (21)–(25). Beam displacements are approximated by functions

$$\bar{w}_1(x) = w_1(x, 1) = w_3(x, -1) = \sum \bar{W}_n^1 \psi_{2n}(x); \quad \bar{u}_1(x) = u_1(x, 1) = u_3(x, -1) = \sum \bar{U}_n^1 P_{2n+1}(x). \tag{29a}$$

For the last plate in Model 3 (Fig. 4,c), the approximation of the displacement functions has the form

$$w_1(x, y) = \sum \sum W_{ij}^1 \psi_{2n}(x) \eta_{2n}(y); \quad u_1(x, y) = \sum \sum \bar{U}_{ij}^1 P_{2i+1}(x) P_{2j}(y); \quad v_1(x, y) = \sum \sum \bar{V}_n^1 P_{2i}(x) P_{2j+1}(y). \tag{29b}$$

Here, symmetry is considered, and the form of functions  $\eta_i(y)$  is presented in (4).

The unknown coefficients that determine three problems solutions of structural deformation are found from a system of linear algebraic equations, which can be found from the condition for the minimum of the total potential energy:

– for Model 1:

$$\sum_{i=1,2,3} [\delta \Pi_\varepsilon^b(w_i) + \delta \Pi_\varepsilon^p(u_i, v_i)] = qab \int_{-1}^1 \int_{-1}^1 [\delta w_1 + \delta w_3] dx dy; \tag{30}$$

– for Model 2:

$$\sum_{i=1,3} [\delta \Pi_\varepsilon^b(w_i) + \delta \Pi_\varepsilon^p(u_i, v_i)] + \delta \bar{\Pi}_\varepsilon^b(\bar{u}_1, \bar{w}_1) = qab \int_{-1}^1 \int_{-1}^1 [\delta w_1 + \delta w_3] dx dy; \tag{31}$$

– for Model 3:

$$\delta \Pi_\varepsilon^b(w_1) + \delta \Pi_\varepsilon^p(u_1, v_1) + \delta \bar{\Pi}_\varepsilon^b(\bar{u}_1, \bar{w}_1) = 2qab \int_{-1}^1 \int_{-1}^1 \delta w_1 dx dy. \tag{32}$$

The implementation of the calculation for Model 1, performed in the Maple system, is given in the Appendix.

It should be noted here that Model 1 and Models 2 and 3 describe slightly different problems. If in Model 1 inhomogeneous displacement of points  $x = \pm 1$  and  $y = -1$  of plate 2 is allowed, then in Models 2 and 3 these points can be displaced along the x-axis without rotation.

Note also that the built approximations of the displacement functions (19), (21)–(25), (27) or (28) for the Model 1, (19), (21)–(25), (29) for the Model 2, and (30) for the Model 3 exactly satisfy all the essential boundary and conjugation conditions. The definition of unknown coefficients included in these approximations depends on the type of the problem being solved, i.e. on the form of functionals (11)–(13) and right-hand sides in (30)–(32). Here (30)–(32) correspond to static analysis. There is nothing to prevent the use of these approximations (possibly abandoning symmetry) for other problems as well. For example, replacing the right-hand sides with inertial terms in (30)–(32), we come to a modal analysis. If placed the action of the initial state on the displacements of the perturbed in the right-hand sides, we come to a buckling analysis. The anisotropy of material properties will affect only the form of functionals (11)–(13). Replacing them with nonlinear analogs will allow solving physically and geometrically nonlinear problems, etc.

### 3. The Results of Calculations, Accuracy and Convergence

The following values were compared (Fig. 6): energy of deformation  $\Pi_\varepsilon$ , maximum deflection  $w_{max}$ , displacement  $u$  along the x-axis, extremum of the bending moment  $M_y$ , shear force  $Q_y$ , and stress  $\sigma_x$ .

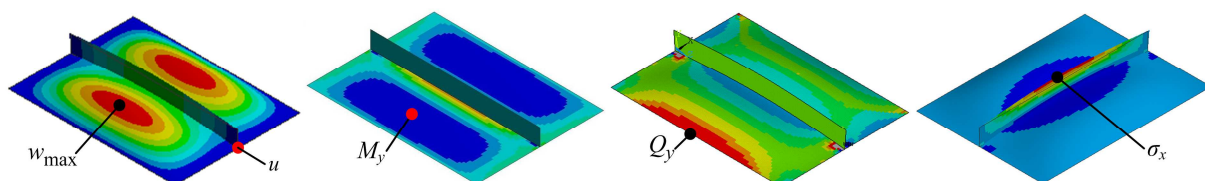


Fig. 6. Places where the comparison values were calculated.





**Table 4.** Reference values for displacements, stresses and their equivalents.

Value	Units	The spectral solution, this paper		FEM (ANSYS, Nastran)		The relative difference, %	
		Model 1	Model 2	Model 1	Model 2	Model 1	Model 2
$N$	pcs.	1065	748	2042601	721401		
$\Pi_z$	N-mm	11856.58	8268.605	11862.60	8276.888	0.05	0.10
$w_{\max}$	mm	2.181512	1.687926	2.182332	1.689024	0.04	0.07
$u$	mm	0.04634379	0.021024375	0.0465343	0.0214378	0.41	1.97
$M_y$	N	326.4823	313.4164	326.5535	313.4537	0.02	0.01
$Q_y$	N/mm	5.926405	5.859336	5.817991	5.656907	1.86	3.45
$\sigma_x$	MPa	80.70894	14.82106	80.74431	14.87589	0.044	0.37

The reference values are given in Table 4. It also indicates the number of unknowns (the order of the solution matrix)  $N$ , wherein the reference value is obtained, and the relative difference between the spectral solution and the FE-solution. It can be seen that the spectral solution and the FE-solution practically coincide. The largest difference is observed in the shear force (almost 2% for Model 1 and more than 3% for Model 2) and displacement  $u$  for Model 2 (almost 2%). These differences are caused by poor convergence of cross force and displacement (Fig. 7, 8). The rest values do not differ by more than 0.5%.

The relative errors in the determination of the noted quantities decrease with an increase in the number of terms in the sums (19), (21)–(25), (27)–(30). As a first approximation, sums with one term were taken. Then the number of terms in each sum increased by one. Thus, the total number of unknowns (matrix order)  $N$  for Model 1 increased as  $N = 25 + 24K + 8K^2$  (25, 57, ..., 889, 1065), for Model 2 –  $N = 8 + 14K + 6K^2$  (8, 28, ..., 620, 748), for Model 3 –  $N = 3(K + 1)^2$  (3, 12, ..., 300, 363). Here  $K = 0, 1, \dots, 10$  is the upper limit of summation. The results at  $K = 10$  are taken as reference ones (Table 4).

To assess the convergence of the FEM, the element size was decreased. The initial size of the rectangular element was taken equal to 80 mm (stringer height). Then the element size decreased (mm): 80, 65, 50, 40, 20, 10, 5, 2. To build the graphs (Fig. 7, 8), the number of nodal unknowns (the size of the stiffness matrix)  $N$  was calculated. In the case of using elements of the first order, row  $N$ , corresponding to a number of element sizes, is as follows: 517, 765, 1209, 1993, 7341, 29081, 115761, 721401, and in the case of elements with intermediate nodes –  $N$ : 1417, 2059, 3469, 5533, 20661, 82121, 327441, 2042601. The results obtained on a mesh with an element size of 2 mm are taken as reference ones (Table 4).

In Fig. 7 shown the convergence of the noted values for Model 1. The results were obtained by SM and FEM using elements of the first and second orders. As it can be seen, the spectral solution has exponential convergence. With the same accuracy, the number of unknowns in the spectral solution is two orders of magnitude less than in the FEM. For all methods, convergence worsens with the increasing order of the derivative. The best convergence has the value  $\Pi_z$  of the energy, the slowest – the shear force  $Q_y$  value (the third derivative of the deflection function). It should be noted that increasing the order of finite elements, in this case, does not lead to more accurate results.

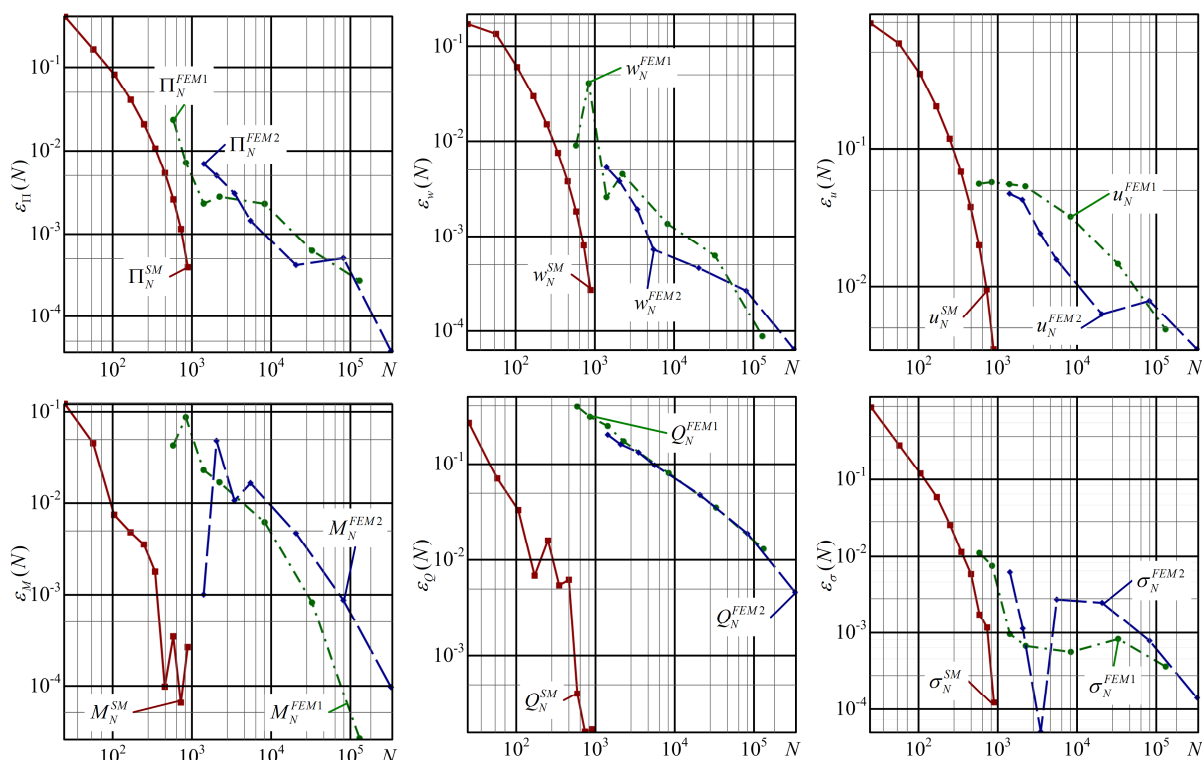


**Fig. 7.** Convergence of deformation energy  $\Pi_z$ , maximum deflection  $w_{\max}$ , displacement  $u$ , extremum of bending moment  $M_y$ , shear force  $Q_y$ , and stress  $\sigma_x$ , calculated by the SM (superscript "SM") and by FEM using elements of the first (superscript "FEM1") and second (superscript "FEM2") orders.



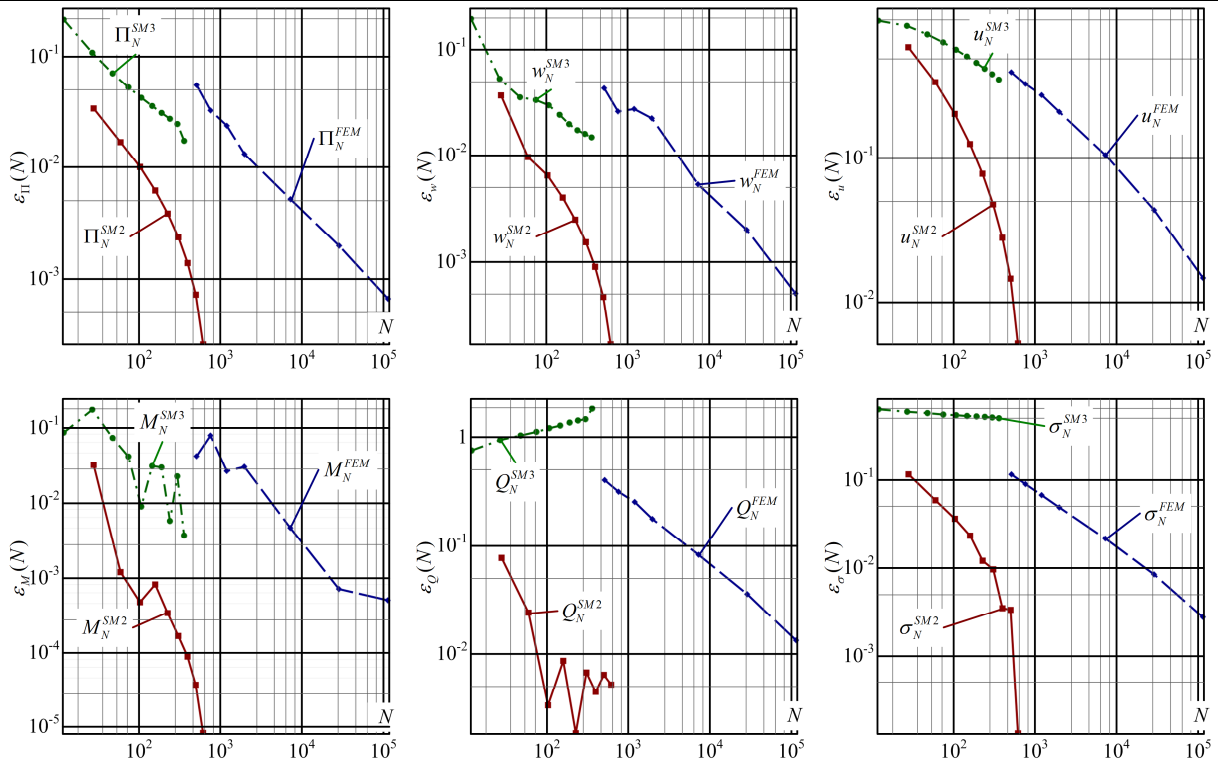


Fig. 8. Convergence of deformation energy  $\Pi$ , maximum deflection  $w_{max}$ , displacement  $u$ , extremum of bending moment  $M_y$ , shear force  $Q_y$ , and stress  $\sigma_x$ , calculated by the SM for Model 2 (superscript “SM2”), for Model 3 (superscript “SM3”), and FEM using first-order elements.

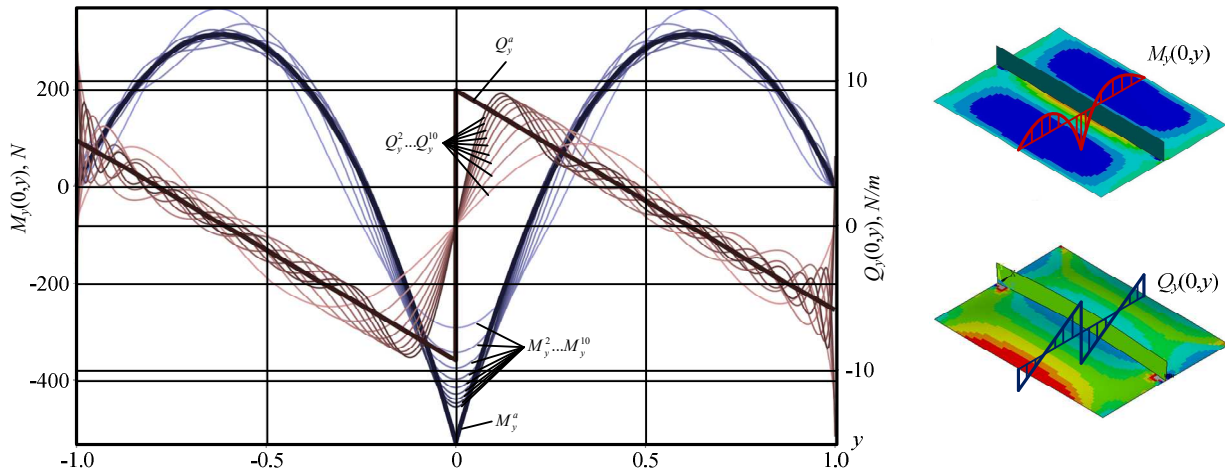


Fig. 9. Gibbs phenomenon due to the approximation functions of the bending moment  $M_y$  and shear force  $Q_y$  on the section  $x = 0$  in the Model 3.

Fig. 8 shows the convergence of the same values in the models of panels with a beam: Model 2 (Fig. 4,b) is denoted by the superscript “SM2”, and Model 3 (Fig. 4,c) by superscript “SM3”. It can be seen that the convergence of the results for the “two plates and a beam” model (SM2) continues exponential, the model with one plate (SM3) does not have such convergence. This is because the second derivative of the function of deflection (bending moment  $M_y$ ) and the third derivative (shear force  $Q_y$ ) have discontinuities on the section where the beam is located. These discontinuities instigate the occurrence of the Gibbs phenomenon.

In Fig. 9 shown the graphs of the distribution of the shear force  $Q_y$  and the bending moment  $M_y$  along the section  $x = 0$  for the model with one plate (SM3). The subscripts indicate the upper limit of the summation in (30). The Gibbs phenomenon arises because the function  $w_1(30)$  at  $x = const$  and all of its derivatives have no discontinuities (belongs to  $C^\infty$ ), and such a discontinuity should be present in the third derivatives (transverse forces). This phenomenon does not arise for the model with two plates (SM2) as well as for the first model with three plates (SM1), since the matching conditions for the plates imply smoothness along the boundary of only the function itself and its first derivative ( $C^1$  – continuity condition between the elemental faces), the rest of the derivatives can have discontinuities, and if such a discontinuity occurs, then it will be approximated exactly. In Fig. 9 the bending moment  $M_y$  and shear force  $Q_y$  obtained in Model 2 are denoted by the subscript “a”.

The Gibbs phenomenon significantly worsens the convergence of energy, displacements of the first (angles of rotation) and second derivatives (bending moments) and leads to its absence for the third derivatives (shear force). If compare the convergence of the model with two plates (SM2) and the FE solution (FEM) (Fig. 8), then, as in the previous example, SM2 retains exponential convergence and allows one to obtain the result with the same accuracy as the FEM, but with the 10–100 times less number of unknowns.



## 4. Conclusion

In this paper, a method for using SM for the analysis of branched thin-walled structures was proposed. The problem that arises when conjugating classic thin rectangular plates, which are in a plane stress state and bend, has been solved. The solution to the problem was presented in two ways: (i) by restructuring the “boundary” basis functions (27); (ii) a representation of a function from  $H^1$  by a basis from  $H^2$ , but with free parameters in the “boundary” functions (28). In addition, a basis systems that satisfies not only the essential but also the natural boundary conditions were constructed. Their use made it possible to increase the convergence rate of approximate solutions. The proposed methods and basis systems were tested on a three-plate structure. Three models of this structure were built: Model 1 – three plates; Model 2 – two plates and a beam; Model 3 – one plate and beam. The reliability of the results was confirmed by comparing them with the FEM solution. The discrepancy does not exceed 3% in terms of stresses and 0.5% in displacements. Numerical calculations have shown that, for Models 1 and 2, the exponential convergence characteristic of SM is retained, but for Model 3 it is not. It is shown that the reason for the deterioration in convergence is the appearance of the Gibbs phenomenon. For Models 1 and 2, engineering accuracy is achieved with the addition of about 100 degrees of freedom, which is orders of magnitude less than in FEM.

It was noted that the bending moment (Fig. 7), shear force (Fig. 7, 8), with an increase in the number of unknowns, cease to be refined, which is associated with an increase in the condition number of the stiffness matrix and the accumulation of round-off errors. This is a known problem for SM and has not been defined in this paper. The situation can be significantly improved if the normalized basis functions are used in the expansions of the displacement functions (here the normalization of the functions was not carried out). Other ways of solving this problem may be a topic for future research.

## Author Contributions

All authors made a substantial, direct, and intellectual contribution to this research. The manuscript was written through the contribution of all authors. All authors discussed the results, reviewed, and approved the final version of the manuscript.

## Acknowledgments

The authors would like to thank the editor and anonymous reviewers for their careful reading of the paper and constructive and valuable comments.

## Conflict of Interest

The authors declared no potential conflicts of interest concerning the research, authorship, and publication of this article.

## Funding

This research is supported by the Ministry of Education and Science of Ukraine as a part of the scientific research project No. 0121U109639.

## Data Availability Statements

The datasets generated and/or analyzed during the current study are available from the corresponding author on reasonable request.

## References

- [1] Kurin, M.O. Determination of the boundaries of plastic zone of metal deformation during the cutting, *Progress in Physics of Metals*, 21(2), 2020, 249–273.
- [2] Plankovskyy, S., Shypul, O., Tsegelnyk, Y., Tryfonov, O., Golovin, I. Simulation of surface heating for arbitrary shape's moving bodies/sources by using R-functions, *Acta Polytechnica*, 56(6), 2016, 472–477.
- [3] Kondratiev, A., Kovalenko, V., Tsaritsynskyi, A., Nabokina, T. Modeling of failure in laminated plates by delamination buckling, *Advanced Manufacturing Processes II*, LNME, pp. 149–158, Springer, 2021.
- [4] Shypul, O., Myntiuk, V. Transient thermoelastic analysis of a cylinder having a varied coefficient of thermal expansion, *Periodica Polytechnica Mechanical Engineering*, 64(4), 2020, 273–278.
- [5] Ferretti, M., D'Annibale, F., Luongo, A. Modeling beam-like planar structures by a one-dimensional continuum: an analytical-numerical method, *Journal of Applied and Computational Mechanics*, 7, 2021, 1020–1033.
- [6] Dlamini, P., Simelane, S. An efficient spectral method-based algorithm for solving a high-dimensional chaotic Lorenz system, *Journal of Applied and Computational Mechanics*, 7(1), 2021, 225–234.
- [7] Boyd, J.P. *Chebyshev and Fourier Spectral Methods*, Dover Publications, Mineola, NY, 2000.
- [8] Shen, J., Tang, T., Wang, L.L. *Spectral Methods*, SSCM, vol. 41, Springer, Berlin, Heidelberg, 2011.
- [9] Babuska, I., Szabo, B.A., Katz, I.N. The  $p$ -version of the finite element method, *SIAM Journal on Numerical Analysis*, 18(3), 1981, 515–545.
- [10] Patera, A.T. A spectral element method for fluid dynamics: laminar flow in a channel expansion, *Journal of Computational Physics*, 54(3), 1984, 468–488.
- [11] Montigny-Rannou, F., Morchoisne, Y. A spectral method with staggered grid for incompressible Navier-Stokes equations, *International Journal for Numerical Methods in Fluids*, 7(2), 1987, 175–189.
- [12] Streett, C.L. Spectral methods and their implementation to solution of aerodynamic and fluid mechanic problems, *International Journal for Numerical Methods in Fluids*, 7(11), 1987, 1159–1189.
- [13] Kopriva, D.A. Domain decomposition with both spectral and finite difference methods for the accurate computation of flows with shocks, *Applied Numerical Mathematics*, 6(1-2), 1989, 141–151.
- [14] Muñoz, R. Theoretical analysis of some spectral multigrid methods, *Computer Methods in Applied Mechanics and Engineering*, 80(1-3), 1990, 287–294.
- [15] Babuška, I., Suri, M. The  $p$ - and  $h$ - $p$  versions of the finite element method, an overview, *Computer Methods in Applied Mechanics and Engineering*, 80(1-3), 1990, 5–26.
- [16] Babuška, I., Li, L. The  $h$ - $p$ -version of the finite-element method in the plate modelling problem, *Communications in Applied Numerical Methods*, 8(1), 1992, 17–26.
- [17] Carlenzoli, C., Gervasio, P. Effective numerical algorithms for the solution of algebraic systems arising in spectral methods, *Applied Numerical Mathematics*, 10(2), 1992, 87–113.
- [18] Jensen, S., Suri, M. On the  $L_2$  error for the  $p$ -version of the finite element method over polygonal domains, *Computer Methods in Applied Mechanics and Engineering*, 97(2), 1992, 233–243.
- [19] Ahmed, N.U., Basu, P.K. Higher order modeling of plates by  $p$ -version of finite element method, *Journal of Engineering Mechanics*, 119(6), 1993, 1228–1242.
- [20] Karageorghis, A. Conforming Chebyshev spectral methods for Poisson problems in rectangular domains, *Journal of Scientific Computing*, 8(2), 1993,



123–133.

- [21] Pavarino, L.F. Additive Schwarz methods for the  $p$ -version finite element method, *Numerische Mathematik*, 66(1), 1993, 493–515.
- [22] Fish, J., Guttal, R. Recent advances in the  $p$ -version of the finite element method for shells, *Computing Systems in Engineering*, 6(3), 1995, 195–211.
- [23] Kumar, K.K., Eswaran, V. A fully spectral solution method for parabolic equations, *Communications in Numerical Methods in Engineering*, 11(9), 1995, 765–774.
- [24] Pavarino, L.F., Widlund, O.B. Iterative substructuring methods for spectral elements: Problems in three dimensions based on numerical quadrature, *Computers & Mathematics with Applications*, 33(1-2), 1997, 193–209.
- [25] Warburton, T.C., Lomtev, I., Du, Y., Sherwin, S.J., Karniadakis, G.E. Galerkin and discontinuous Galerkin spectral/ $h$ - $p$  methods, *Computer Methods in Applied Mechanics and Engineering*, 175(3-4), 1999, 343–359.
- [26] Babuška, I., Griebel, M., Pitkäranta, J. The problem of selecting the shape functions for a  $p$ -type finite element, *International Journal for Numerical Methods in Engineering*, 28(8), 1989, 1891–1908.
- [27] Kurtz, J., Xenophontos, C. On the effects of using curved elements in the approximation of the Reissner-Mindlin plate by the  $p$  version of the finite element method, *Applied Numerical Mathematics*, 46(2), 2003, 231–246.
- [28] Houmat, A. Free vibration analysis of membranes using the  $h$ - $p$  version of the finite element method, *Journal of Sound and Vibration*, 282(1-2), 2005, 401–410.
- [29] Rieutord, M., Dubrulle, B., Grandclément, P. Introduction to spectral methods, *European Astronomical Society Publications Series*, 21, 2006, 153–180.
- [30] Hill, A.A., & Straughan, B. A Legendre spectral element method for eigenvalues in hydrodynamic stability, *Journal of Computational and Applied Mathematics*, 193(1), 2006, 363–381.
- [31] Houmat, A. Three-dimensional free vibration analysis of plates using the  $h$ - $p$  version of the finite element method, *Journal of Sound and Vibration*, 290(3-5), 2006, 690–704.
- [32] Houmat, A. Free vibration analysis of arbitrarily shaped membranes using the trigonometric  $p$ -version of the finite-element method, *Thin-Walled Structures*, 44(9), 2006, 943–951.
- [33] Mai-Duy, N., Tanner, R.I. A spectral collocation method based on integrated Chebyshev polynomials for two-dimensional biharmonic boundary-value problems, *Journal of Computational and Applied Mathematics*, 201(1), 2007, 30–47.
- [34] Bittencourt, M.L., Vazquez, T.G. A nodal spectral stiffness matrix for the finite-element method, *IMA Journal of Applied Mathematics*, 73(6), 2008, 837–849.
- [35] Šolín, P., Vejchodský, T. Higher-order finite elements based on generalized eigenfunctions of the Laplacian, *International Journal for Numerical Methods in Engineering*, 73(10), 2008, 1374–1394.
- [36] Auteri, F., Quartapelle, L. Galerkin–Legendre spectral method for the 3D Helmholtz equation, *Journal of Computational Physics*, 161(2), 2000, 454–483.
- [37] Hadjoui, A., Mebarek, H., Bouiadjra, B.B. Free vibration analysis for cracked triangular orthotropic plates using  $h$ - $p$  finite element method, *International Journal for Computational Methods in Engineering Science and Mechanics*, 12(2), 2011, 59–74.
- [38] Zheng, X., Dong, S. An eigen-based high-order expansion basis for structured spectral elements, *Journal of Computational Physics*, 230(23), 2011, 8573–8602.
- [39] Sari, M.E.S., Butcher, E.A. Free vibration analysis of rectangular and annular Mindlin plates with undamaged and damaged boundaries by the spectral collocation method, *Journal of Vibration and Control*, 18(11), 2012, 1722–1736.
- [40] Ai, Q., Li, H., Wang, Z. Diagonalized Legendre spectral methods using Sobolev orthogonal polynomials for elliptic boundary value problems, *Applied Numerical Mathematics*, 127, 2018, 196–210.
- [41] Wang, T., Sun, T. Galerkin–Legendre spectral method for Neumann boundary value problems in three dimensions, *International Journal of Computer Mathematics*, 96(7), 2019, 1335–1356.
- [42] Li, S., Li, Q., Wang, Z. Sobolev orthogonal Legendre rational spectral methods for problems on the half line, *Mathematical Methods in the Applied Sciences*, 43(1), 2020, 255–268.
- [43] Oh, S. An efficient spectral method to solve multi-dimensional linear partial differential equations using Chebyshev polynomials, *Mathematics*, 7(1), 2019, 90.
- [44] Lotfi, M., Alipanah, A. Legendre spectral element method for solving Volterra-integro differential equations, *Results in Applied Mathematics*, 7, 2020, 100116.
- [45] Katz, I.N., Wang, D.W. The  $p$ -version of the finite element method for problems requiring  $C^1$ -continuity, *SIAM Journal on Numerical Analysis*, 22(6), 1985, 1082–1106.
- [46] Lindsay, K.A., Ogden, R.R. A practical implementation of spectral methods resistant to the generation of spurious eigenvalues, *International Journal for Numerical Methods in Fluids*, 15(11), 1992, 1277–1294.
- [47] Bardell, N.S., Dunsdon, J.M., Langley, R.S. Free vibration analysis of thin rectangular laminated plate assemblies using the  $h$ - $p$  version of the finite element method, *Composite Structures*, 32(1-4), 1995, 237–246.
- [48] Lee, U., Jeon, D. Identification of non-ideal structural boundary conditions by using spectral element method, *40th Structures, Structural Dynamics, and Materials Conference and Exhibit*, St. Louis, MO, USA, AIAA-99-1311, 1999.
- [49] Khalilov, S.A. Solution in a rectangle of theory of elasticity static problem at stresses given on the boundary, *Design Issues of Aircraft Structures*, 3, 1982, 120–127. [in Russian]
- [50] Bialecki, B., Karageorghis, A. A Legendre spectral Galerkin method for the biharmonic Dirichlet problem, *SIAM Journal on Scientific Computing*, 22(5), 2001, 1549–1569.
- [51] Muradova, A.D., Stavroulakis, G.E. Buckling and postbuckling analysis of rectangular plates resting on elastic foundations with the use of the spectral method, *Computer Methods in Applied Mechanics and Engineering*, 205, 2012, 213–220.
- [52] Wang, G., Unal, A. Free vibration of stepped thickness rectangular plates using spectral finite element method, *Journal of Sound and Vibration*, 332(18), 2013, 4324–4338.
- [53] Khan, A., Husain, A. Exponentially accurate spectral element method for fourth order elliptic problems, *Journal of Scientific Computing*, 71(1), 2017, 303–328.
- [54] Zhuang, Q., Chen, L. Legendre–Galerkin spectral-element method for the biharmonic equations and its applications, *Computers & Mathematics with Applications*, 74(12), 2017, 2958–2968.
- [55] Sze, K.Y., Hu, Y.C. Assumed natural strain and stabilized quadrilateral Lobatto spectral elements for  $C^0$  plate/shell analysis, *International Journal for Numerical Methods in Engineering*, 111(5), 2017, 403–446.
- [56] Liu, X., Banerjee, J.R. Free vibration analysis for plates with arbitrary boundary conditions using a novel spectral-dynamic stiffness method, *Computers & Structures*, 164, 2016, 108–126.
- [57] Tkachenko, D.A. Orthonormal basis in the biharmonic operator energy space in the rectangle with homogeneous principal boundary conditions along the boundary, *Aerospace Technic and Technology*, 3, 2014, 41–51. [in Russian]
- [58] Khalilov, S.A., Myntiuk, V.B., Tkachenko, D.A., Kopychko, V.V. Biharmonic operator own spectrum in a rectangle at the main boundary conditions, *Aerospace Technic and Technology*, 5, 2014, 70–78. [in Russian]
- [59] Kravchenko, S.G., Myntiuk, V. Nonlinear postbuckling behavior of a simply supported, uniformly compressed rectangular plate, *Integrated Computer Technologies in Mechanical Engineering*, AISC, vol. 1113, pp. 35–44, Springer, Cham, 2020.
- [60] Myntiuk, V.B. Postbuckling of a uniformly compressed simply supported plate with free in-plane translating edges, *Journal of Applied and Industrial Mathematics*, 14(1), 2020, 176–185.
- [61] Khalilov, S.A., Myntiuk, V.B. Postbuckling analysis of flexible elastic frames, *Journal of Applied and Industrial Mathematics*, 12(1), 2018, 28–39.
- [62] Freud, G. *Orthogonal Polynomials*, Elsevier Science, Burlington, 2014.
- [63] Szabó, B., Babuška, I. *Finite Element Analysis*, John Wiley & Sons, New York, 1991.
- [64] Shen, J. Efficient spectral-Galerkin method I. Direct solvers of second- and fourth-order equations using Legendre polynomials, *SIAM Journal on Scientific Computing*, 15(6), 1994, 1489–1505.
- [65] Timoshenko, S., Woinowsky-Krieger, S. *Theory of Plates and Shells*, McGraw-Hill Education, New Delhi, 2015.
- [66] Myntiuk, V.B. Orthonormal basis for one-dimensional boundary value problems, *Aerospace Technic and Technology*, 5, 2007, 32–36. [in Russian]
- [67] Bardell, N.S., Dunsdon, J.M., Langley, R.S. Free vibration analysis of thin rectangular laminated plate assemblies using the  $h$ - $p$  version of the finite element method, *Composite Structures*, 32(1-4), 1995, 237–246.
- [68] Kombarov, V., Sorokin, V., Tsegelnyk, Y., Plankovskyy, S., Aksonov, Y., Fojtů, O. Numerical control of machining parts from aluminum alloys with



sticking minimization, *International Journal of Mechatronics and Applied Mechanics*, 1(9), 2021, 209–216.

[69] Krivtsov, V.S., Voronko, V.V., Zaytsev, V.Y. Advanced prospects for the development of aircraft assembly technology, *Science and Innovation*, 11(3), 2015, 11–18.

[70] Sikulskiy, V., Sikulskiy, S., Garin, V. Investigation into the forming process of wing panel oblique bending by means of rib rolling, *Integrated Computer Technologies in Mechanical Engineering – 2020*. LNNS, vol. 188, pp. 598–608, Springer, Cham, 2021.

[71] Plankovskyy, S., Myntiuk, V., Tsegelnyk, Y., Zadorozhnyi, S., Kombarov, V. Analytical methods for determining the static and dynamic behavior of thin-walled structures during machining, *Mathematical Modeling and Simulation of Systems (MODS'2020)*, AISC, vol. 1265, pp. 82–91, Springer, Cham, 2021.

[72] Zhou, W., Li, Y., Shi, Z., Lin, J. An analytical solution for elastic buckling analysis of stiffened panel subjected to pure bending, *International Journal of Mechanical Sciences*, 161, 2019, 105024.


## Appendix


```
restart; with(LinearAlgebra): with(orthopoly): unprotect(D): unprotect(order):
# MPa, mm
nu:=3/10; E:=72000; G:=E/(2*(1+nu));
# dimensions
a:=800/2; b:=[300/2,80/2,300/2]; h:=[6,8,6]; pressure:=5/100;
D:=[seq(E*h[i]^3/(12*(1-nu^2)),i=1..nops(h))]; A:=[seq(E*h[i]/(1-nu^2),i=1..nops(h))];
M:=2;N:=M; N1:=(x)->(P(0,x)-P(1,x))/2; N2:=(x)->(P(0,x)+P(1,x))/2;
M1:=(x)->1/2*P(0,x)-3/5*P(1,x)+1/10*P(3,x); M2:=(x)->1/2*P(0,x)+3/5*P(1,x)-1/10*P(3,x);
K1:=(x)->(1/6*P(0,x)-1/10*P(1,x)-1/6*P(2,x)+1/10*P(3,x));#a/2;
K2:=(x)->(1/6*P(0,x)-1/10*P(1,x)+1/6*P(2,x)+1/10*P(3,x));#a/2;
M1_:=:(x)->((x-1)*(x^2-2*x-11))/16; M2_:=:(x)->-((x+1)*(x^2+2*x-11))/16;
phi:=(i,x)->P(i+2,x)-P(i,x); phi_of:=(i,x)->P(i+1,x)+P(i,x); phi_f0:=(i,x)->P(i+1,x)-P(i,x);
psi:=(n,x)->P(n+4,x)-2*(2*n+5)/(2*n+3)*P(n+2,x)+(2*n+7)/(2*n+3)*P(n,x);
psi_sc:=(n,x)->P(n+4,x)+(2*n+7)*P(n+3,x)/(n+2)^2-(2*n+5)*(2*n+1)^2+6*n+13)*P(n+2,x)/((2*n+3)*(n+2)^2-
(2*n+7)*P(n+1,x)/(n+2)^2+(n+3)^2*(2*n+7)*P(n,x)/((2*n+3)*(n+2)^2);
psi_cs:=(n,x)->P(n+4,x)-(2*n+7)*P(n+3,x)/(n+2)^2-(2*n+5)*(2*n+1)^2+6*n+13)*P(n+2,x)/((2*n+3)*(n+2)^2
+(2*n+7)*P(n+1,x)/(n+2)^2+(n+3)^2*(2*n+7)*P(n,x)/((2*n+3)*(n+2)^2);
w1:=sum(psi(2*n,x)*W_1[n]*M2_(y),n=0..M)+sum(sum(W1[i,j]*psi(2*i,x)*psi_sc(j,y),i=0..M),j=0..N):
u1:=sum(P(2*n+1,x)*U_1[n]*N2(y),n=0..M)+sum(sum(U1[i,j]*P(2*i+1,x)*phi_f0(j,y),i=0..M),j=0..N):
v1:=sum(sum(V1[i,j]*P(2*i,x)*phi_f0(j,y),i=0..M),j=0..N):
V1_:=:(i)->piecewise(i<1,-(2*i+7)/(2*i+3)*W_1[i/2],i<=2*M,W_1[(i-2)/2]-(2*i+7)/(2*i+3)*W_1[i/2],W_1[(i-2)/2]);
w2:=0:
u2:=sum(P(2*n+1,x)*U_1[n]*N1(y),n=0..M)+sum(sum(U2[i,j]*P(2*i+1,x)*phi_of(j,y),i=0..M),j=0..N):
v2:=0*N1(x)*N1(y)+0*N2(x)*N1(y)+v_3*N1(x)*N2(y)+v_4*N2(x)*N2(y)+N1(y)*sum(V1_(2*n)*phi(2*n,x),n=0..M+1)+N2(y)*sum(V_2[n]*p
hi(2*n,x),n=0..M+1)+N1(x)*sum(V_4[n]*phi(n,y),n=0..N+2)+N2(x)*sum(V_3[n]*phi(n,y),n=0..N+2)+sum(sum(V2[i,j]*phi(2*i,x)*phi(j,y),i=
0..M+1),j=0..N+2):
w3:=sum(psi(2*n,x)*W_1[n]*M1_(y),n=0..M)+sum(sum(W3[i,j]*psi(2*i,x)*psi_cs(j,y),i=0..M),j=0..N):
u3:=sum(P(2*n+1,x)*U_1[n]*N1(y),n=0..M)+sum(sum(U3[i,j]*P(2*i+1,x)*phi_of(j,y),i=0..M),j=0..N):
v3:=sum(sum(V3[i,j]*P(2*i,x)*phi_of(j,y),i=0..M),j=0..N):
Unk:=[]
#Node
v_3,v_4,
#beam
seq(W_1[n],n=0..M),seq(U_1[n],n=0..M), seq(V_2[n],n=0..M+1),seq(V_3[n],n=0..N+2),seq(V_4[n],n=0..N+2),
#plate
seq(seq(W1[i,j],i=0..M),j=0..N),seq(seq(U1[i,j],i=0..M),j=0..N),seq(seq(V1[i,j],i=0..M),j=0..N),
seq(seq(U2[i,j],i=0..M),j=0..N),seq(seq(V2[i,j],i=0..M+1),j=0..N+2),
seq(seq(W3[i,j],i=0..M),j=0..N),seq(seq(U3[i,j],i=0..M),j=0..N),seq(seq(V3[i,j],i=0..M),j=0..N)
]:
order:=nops(Unk);
Energ:=expand
(D[1]/2*a*b[1]*int(int(1/a^4*diff(w1,x,x)^2+1/b[1]^4*diff(w1,y,y)^2+1/(a^2*b[1]^2)*(2*nu*diff(w1,x,x)*diff(w1,y,y)+2*(1-
nu)*diff(w1,x,y)^2),x=-1..1),y=-1..1)+D[2]/2*a*b[2]*int(int(1/a^4*diff(w2,x,x)^2+
1/b[2]^4*diff(w2,y,y)^2+1/(a^2*b[2]^2)*(2*nu*diff(w2,x,x)*diff(w2,y,y)+2*(1-nu)*diff(w2,x,y)^2),x=-1..1),y=-
1..1)+D[3]/2*a*b[3]*int(int(1/a^4*diff(w3,x,x)^2+1/b[3]^4*diff(w3,y,y)^2+1/(a^2*b[3]^2)*(2*nu*diff(w3,x,x)*diff(w3,y,y)+2*(1-
nu)*diff(w3,x,y)^2),x=-1..1),y=-1..1)+1/2*A[1]*a*b[1]*int(int((1/a*diff(u1,x)+1/b[1]*diff(v1,y))^2+(1-
nu)/2*((1/b[1]*diff(u1,y)+1/a*diff(v1,x))^2-4*(1/a*b[1])*diff(v1,y)*diff(u1,x)),x=-1..1),y=-1..1)+1/2*A[2]*a*b[2]*int(int((1/a*diff(u2,x)+
1/b[2]*diff(v2,y))^2+(1-nu)/2*((1/b[2]*diff(u2,y)+1/a*diff(v2,x))^2-4*(1/a*b[2])*diff(v2,y)*diff(u2,x)),
x=-1..1),y=-
1..1)+1/2*A[3]*a*b[3]*int(int((1/a*diff(u3,x)+1/b[3]*diff(v3,y))^2+(1-nu)/2*((1/b[3]*
diff(u3,y)+1/a*diff(v3,x))^2-
4*(1/a*b[3])*diff(v3,y)*diff(u3,x)),x=-1..1),y=-1..1)-pressure*a*b[1]*int(int(w1,x=-1..1),y=-1..1)-pressure*a*b[3]*int(int(w3,x=-1..1),y=-1..1)
):
Eq:=seq(diff(Energ,Unk[i]),i=1..order):
(R,r):=GenerateMatrix(Eq,Unk,shape=symmetric,attributes=[positive_definite]);
Res:=LinearSolve(R,r);
assign(seq(Unk[i]=Res[i],i=1..order)):
y_max:=fsolve(diff(eval(w1,x=0),y),y=-1*0.9..1*0.9);
w_max:=evalf(eval(w1,[x=0,y=y_max])); u_max:=evalf(eval(u1,[x=-1,y=1]));
M1x:=-D[1]*(diff(w1,x,x)/a^2+nu*diff(w1,y,y)/b[1]^2);
M1y:=-D[1]*(diff(w1,y,y)/b[1]^2+nu*diff(w1,x,x)/a^2);
M1xy:=D[1]/(1-nu)*diff(w1,x,y)/b[1]/a;
Q1x:=diff(M1x,x)/a-diff(M1xy,y)/b[1];
Q1y:=diff(M1y,y)/b[1]-diff(M1xy,x)/a;
yM_max:=fsolve(diff(eval(M1y,x=0),y),y=-0.9..0.9);
M_max:=eval(M1y,[x=0,y=yM_max]); Q_fix:=evalf(eval(Q1y,[x=0,y=-1]));
N2x:=A[2]*(diff(u2,x)/a+nu*diff(v2,y)/b[2]);
```





$N2\_max:=evalf(eval(N2x,[x=0,y=1]));$

### ORCID iD

Denys Tkachenko  <https://orcid.org/0000-0002-5006-6775>

Yevgen Tsegelnyk  <https://orcid.org/0000-0003-1261-9890>

Sofia Myntiuk  <https://orcid.org/0000-0003-4581-1176>

Vitalii Myntiuk  <https://orcid.org/0000-0002-4047-0192>



© 2022 Shahid Chamran University of Ahvaz, Ahvaz, Iran. This article is an open access article distributed under the terms and conditions of the Creative Commons Attribution-NonCommercial 4.0 International (CC BY-NC 4.0 license) (<http://creativecommons.org/licenses/by-nc/4.0/>).

**How to cite this article:** Tkachenko D., Tsegelnyk Y., Myntiuk S., Myntiuk V. Spectral Methods Application in Problems of the Thin-Walled Structures Deformation, *J. Appl. Comput. Mech.*, 8(2), 2022, 641–654. <https://doi.org/10.22055/JACM.2021.38346.3207>

**Publisher's Note** Shahid Chamran University of Ahvaz remains neutral with regard to jurisdictional claims in published maps and institutional affiliations.

